Tanzania Journal of Science 46(3): 903-913, 2020
ISSN 0856-1761, e-ISSN 2507-7961

Performance Evaluation of Aspect Dependent-Based Ghost Suppression Methods for Through-the-Wall Radar Imaging

Mugundu Rambika[1,2]*, Abdi T. Abdalla[1], Baraka J. Maiseli[1] and Alfred J. Mwambela[1]
[1]Department of Electronics and Telecommunications Engineering,
College of Information and Communication Technologies, University of Dar es Salaam, P. O. Box 33335, Dar es Salaam, Tanzania.
[2]Tanzania Meteorological Authority, P. O. Box 3056, Dar es Salaam, Tanzania.
**Corresponding author, e-mail: mugundu.rambika@meteo.go.tz*
Co-authors, e-mails: abdit@udsm.ac.tz; barakamaiseli@yahoo.com; nkomo98@yahoo.com
Received 19 Aug 2020, Revised 27 Oct 2020, Accepted 30 Oct 2020, Published Oct 2020
https://dx.doi.org/10.4314/tjs.v46i3.28

Abstract

There are many approaches which address multipath ghost challenges in Through-the-Wall Radar Imaging (TWRI) under Compressive Sensing (CS) framework. One of the approaches, which exploits ghosts' locations in the images, termed as Aspect Dependent (AD), does not require prior knowledge of the reflecting geometry making it superior over multipath exploitation based approaches. However, which method is superior within the AD based category is still unknown. Therefore, their performance comparison becomes inevitable, and hence this paper presents their performance evaluation in view of target reconstruction. At first, the methods were grouped based on how the subarrays were applied: multiple subarray, hybrid subarray and sparse array. The methods were fairly evaluated on varying noise level, data volume and the number of targets in the scene. Simulation results show that, when applied in a noisy environment, the hybrid subarray-based approaches were robust than the multiple subarray and sparse array. At 15 dB signal-to-noise ratio, the hybrid subarray exhibited signal to clutter ratio of 3.9 dB and 4.5 dB above the multiple subarray and sparse array, respectively. When high data volumes or in the case of multiple targets, multiple subarrays with duo subarrays became the best candidates.

Keywords: Aspect dependent, compressive sensing, point target, through-wall-radar imaging

Introduction

Through-the-wall radar imaging (TWRI) is a relatively new research area in radar imaging and signal processing fields. It has recently been gaining attention due to its capability of detecting objects in obscured areas such as behind-the-wall objects. Its applications are in fire and earthquake rescue missions, reconnaissance, emergency relief operation, and military operations (Gennarelli and Soldovieri 2015, Leigsnering et al. 2016, Jia et al. 2019a, Qu et al. 2019).

In reconstructing the scenes of interest, TWRI is still facing serious challenges, including clutters caused by strong reflections from the front wall and the multipath ghosts due to returns from side and back walls, hence making difficult in scene interpretation (Lim and Nam 2014, Jia et al. 2019a, Tivive et al. 2019, Shi et al. 2020, Tang et al. 2020). The front wall obstructs the transmitted power from the transmitter to reach the intended target and the target return echo to the radar. As a result, the received signal becomes weaker, resulting into missed target detections. The front wall also introduces wall residuals in the reconstructed scene caused by front wall reverberation effect (Leigsnering et al. 2014a, 2014b). The effect caused by the front wall has been addressed using spatial filtering techniques (Yoon and Amin 2009, Yao et al. 2014, Ma et al. 2018). Multipath returns resulting from side wall and back wall reflections pose a serious challenge by introducing ghosts in the reconstructed image. If these ghosts are not suppressed, they will populate the scene, resulting in confusion with genuine targets (Abdalla et al. 2018).

To tackle the ghost suppression problem, early approaches used Back Projection (BP) technique in which full measurements employing all antennas and frequencies are used. The full sensing requirement leads to the burden of data collection and increased acquisition time, thus the approach becomes less effective in many applications (Zhang et al. 2012, Tang et al. 2020). To address these challenges, Compressed Sensing (CS) techniques were used (Lagunas et al. 2012a, Tseng et al. 2017, Yang et al. 2019, Tang et al. 2020). A number of ghost suppression methods under the compressive sensing (CS) framework have been devised in the literature. They are broadly categorized in two main groups: multipath exploitation-based and aspect dependent-based methods. The later does not require complete knowledge of the reflecting geometry, thus making it more practical especially in rescue missions.

In Yan et al. (2016), authors used N non-overlapping subarrays, and each subarray is used to form a sub-image. Then, sub-images are strategically fused to obtain a ghost-free image. In Tan and Song (2010) authors used 8 different subarrays to form the subarray images. Through pixel-wise operation on the subarray images using a trained Markov Model, the target images were obtained. In Muqaibel et al. (2017a), authors developed aspect dependent based multipath ghost suppression technique under CS framework. In their work, duo-subarray was used in which measurements were randomly collected such that the aspect dependent feature is maximized and the corresponding images were then strategically combined to suppress the ghosts. In Muqaibel et al. (2017a), a Pythagorean-based array configuration with sparse reconstruction under aspect dependent features has also been used. This approach has shown to give a better manipulation of the aperture dimensions and ensures a better trade-off between the minimum required number of elements to satisfy the requirement of compressive sensing data volume for correct image reconstruction and image quality. The contribution in Guo et al. (2018) used array rotation to maximize the aspect dependent feature and hence suppress the multipath ghost. The array was rotated at three different angles: -30^{o}, 0^{o}, and 30^{o}. However, the method will be challenged by the front wall mitigation process, which is inevitable in TWRI applications.

Currently, there is no comparative study on the existing ghost suppression methods employing aspect dependent, which is the contribution made by this paper. The paper aims at establishing the best ghost suppression method based on aspect dependent feature under compressive sensing framework.

Materials and Methods

Received signal and scene model

Consider a scene showing possible first-order multipath returns with N different radar locations (Figure 1). At every radar location, M monochromatic waves, which are equally spaced in frequency, are transmitted and received. This setup was used by some other authors in the literature (Leigsnering et al. 2014a, 2014b Muqaibel et al. 2017a, 2017b, Jia et al. 2019a, Jia et al. 2019b).

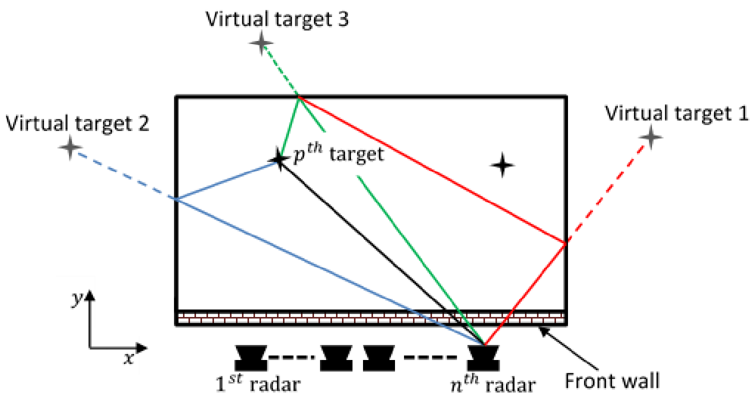

Figure 1: A multipath scenario with first-order returns.

The required scene is then divided into N_x and N_y grid points along the cross-range and down-range directions, respectively. Let σ_p be the target reflectivity for the p^{th} pixel, where $p = 0, 1, \ldots N_x N_y - 1$ and the value of $\sigma_p = 0$ signifies absence of a target, otherwise a target is present in a scene. Thus, if we consider R returns, the target return, $y_t[m, n]$, observed with the n^{th} transceiver when transmitting the m^{th} frequency, f_m, in the presence of a Gaussian noise sample $v(m, n)$, can be expressed as

$$\begin{aligned} y_t[m,n] &= \sum_{r=0}^{R-1} \sum_{p=0}^{N_x N_y - 1} \sigma_p^{(r)} \exp\left(-j2\pi f_m \tau_{pn}^{(r)}\right) \\ &+ \sum_{r_w=0}^{R_w-1} \sigma_w^{(r_w)} \exp\left(-j2\pi f_m \tau_w^{(r_w)}\right) \\ &+ v(m,n). \end{aligned} \tag{1}$$

where $\sigma_p^{(r)}$ and $\sigma_w^{(r_w)}$ represent the target and wall pixel reflectivity, respectively, $\tau_{pn}^{(r)}$ is the round trip delay between p^{th} target, the n^{th} transceiver due to r^{th} return, and $\tau_w^{(r_w)}$ is the time delay of the r_w^{th} front wall return.

The first term on the right-hand side of Equation (1) represents the target return, the second term is the return from the front wall, and the last term is the Gaussian noise component. The target information contained in Equation (1) is analysed in two main approaches to address multipath issues: multipath exploitation, which exploits the multipath returns to eliminate the ghosts (Granström and Bramstång 2019, Qu et al. 2019, Tang and Nguyen 2019, Tang et al. 2020), and aspect dependence (Tan and Song 2010, Yan et al. 2016, Liu et al. 2016, An et al. 2019). Multipath exploitation requires prior knowledge of reflecting geometry which is not always available, thus limiting the application of the method (Jia et al. 2019). Aspect dependent approach considers the fact that ghost locations change with respect to the position of the transceiver (Abdalla et al. 2015, Muqaibel et al. 2017a, Guo et al. 2018). The authors used this peculiar feature to identify and suppress the ghosts. The aspect dependent suppression method is more practical as it does not require complete prior knowledge of the reflecting geometry. Therefore, this work discusses ghost suppression based on aspect dependence feature.

Aspect dependent-based ghost suppression methods

In TWRI, multipath ghosts are aspect dependent, which means that the multipath ghost positions in the reconstructed image change with respect to the transceiver location, while the true target maintains at the same location regardless of the position of the transceiver. The ghosts' pixels have high intensity values over a certain portion of the synthetic aperture, while the true targets' pixels have nearly the same intensity even if the radar location changes, thus making the identification of the ghosts from genuine targets possible (Li et al. 2013, Amin and Ahmad 2014, Tan et al. 2014, Yan et al. 2016, Muqaibel et al. 2017a, Webster et al. 2017, Guo et al. 2018, Jia et al. 2019a, Tang and Nguyen 2019). The point target received signal model in Equation (1) can be expressed in matrix notation as (Abdalla 2018):

$$\boldsymbol{y} = \sum_{r=0}^{R-1} \boldsymbol{\Phi}^{(r)} \boldsymbol{s}^{(r)} + \sum_{r_w=0}^{R_w-1} \boldsymbol{\Phi}_w^{(r)} \boldsymbol{s}_w^{(r_w)} + \boldsymbol{v}, \quad (2)$$

Where $\boldsymbol{s}^{(r)}$ and $\boldsymbol{s}_w^{(r_w)} \in \mathbb{C}^{N_x N_y \times 1}$ are the vector of reflectivities for $r = 0, 1, 2, \ldots R - 1$ and $r_w = 0,1,2, \ldots R_w - 1$

$$\left[\Phi^{(\mathrm{r})}\right]_{\mathrm{ip}} = \exp\left(-j2\pi f_m \tau_{pn}^{(r)}\right) \quad (3)$$

$$\text{and } \left[\Phi_{\mathrm{w}}^{(\mathrm{r})}\right]_{\mathrm{ip}} = \exp\left(-j2\pi f_m \tau_{wn}^{(r_w)}\right) \quad (4)$$

$m = i \bmod M, n = \left\lfloor \frac{i}{M} \right\rfloor, i = 0,1,2,..,MN - 1.$

Expanding Equation (2), and upon factoring out with respect to $\boldsymbol{\Phi}^{(0)}$ and simplifying, we have

$$\boldsymbol{y} = \boldsymbol{\Phi}^{(0)} \tilde{\boldsymbol{s}}^{(0)} + \boldsymbol{v}. \quad (5)$$

From Equation (5), only the direct path information is needed to reconstruct the contaminated scene. If we strategically acquire several contaminated images such that the aspect dependece is pronounced and fuse them, a final image with multipath ghosts suppressed will be reconstructed. To exploit this behaviour, different strategic scene imaging were used. In the literature, we can group these strategies into three different groups, namely multiple subarray, hybrid subarray, and sparse array.

Multiple subarrays

In this category, a full array is subdivided into N subarrays and each is used to interrogate the scene of interest. The ghosts can be easily discriminated as they exhibit aspect dependence in the sub images, which are strategically combined to yield a final image. This category comprises of different methods with varying performances. The authors in Tan and Song (2010) used eight different subarrays and a Hidden Markov Model to suppress ghosts. A similar strategy was also used in Yan et al. (2016). The authors used non-overlapping subarray and an image reconstruction algorithm to reconstruct the scene image. Similar approaches have also been used in Gennarelli and Soldovieri (2015), and in Muqaibel et al. (2017b). The authors in Guo et al. (2018) used a rotatable array during scene imaging. This can as well be grouped in the multiple subarrays category. Each array rotation scan angle is used to form image and these images are fused to obtain the final ghost-free image. Generally, the process of image formation involved in the multiple subarrays category can be summarized as in Figure 2.

Hybrid subarray

There is also a contribution that employs full array measurements and various subarrays to reconstruct the scene image. This group is referred to as *hybrid subarray* because it uses a combination of measurements along the entire array and the measurements from subarrays. Authors in Li et al. (2013) used a combination of a full aperture and duo subarrays. The general ideas in image formation under this category are summarized in Figure 3.

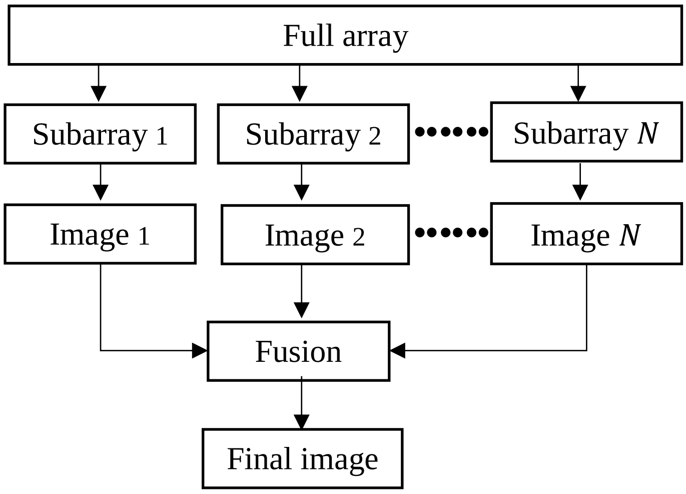

Figure 2: Multiple subarrays image formation.

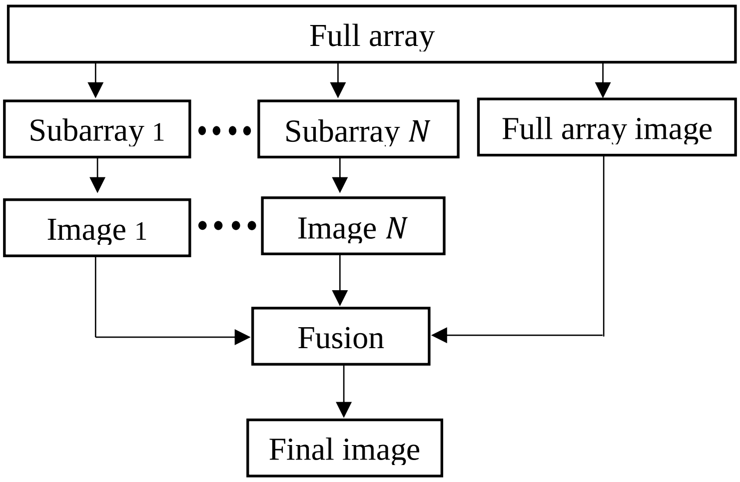

Figure 3 : Hybrid subarray image formation.

Sparse array

Recently, sparse array has emerged as another method to combat multipath effects in TWRI. The Pythagorean based subarray based sparse image reconstruction falls under this category. Authors in Abdalla et al. (2018), Muqaibel et al. (2017b) used Pythagorean-based apertures where N_1, N_2, and N_3 with $N_1 < N_2 < N_3$ are pairwise co-prime integers. In this category, the Pythagorean-based Interlaced Subarray and Pythagorean based Displaced Subarray (PDSA) have shown better performance compared to the other Pythagorean-based approaches. We can generally represent the process of image formation pictorially as in Figure 4.

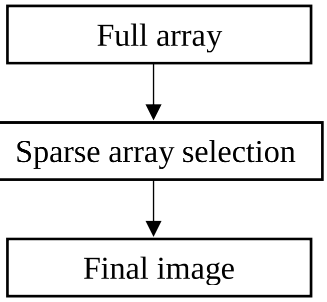

Figure 4: Sparse array image formation.

Experimental setup

In this section, a study of performance evaluation of the aforementioned ghost suppression methods is presented. In each of these methods, MATLAB simulation implementing a stepped frequency monostatic radar was assumed, where the array had 77 array elements linearly spaced at $3.94\, cm$ realizing an array size of $3\ m$ parallel to the front wall. The array was placed 1 m from the front wall. The centre of the array located at (0, 0) was assumed to be the origin of the system. A $2\ GHz$ bandwidth ranging from $1\ GHz$ to $3\ GHz$ was used to realize 201 frequencies spaced at $10\ MHz$. Two-point targets were positioned at $(0.31, 3.6)m$ and $(-0.62, 5.2)m$ inside a room of size $7 \times 6\ m$. The room was assumed to be made of non-reinforced concrete wall with 20 cm wall thickness and relative permittivity of 7.6. Similar wall parameters are used in Jin and Yarovoy (2015), Abdalla and Muqaibel (2016), and Muqaibel et al. (2017a). Four multipath returns were considered. The direct target return, return from the back wall, and the right and left wall returns. The front wall return were mitigated using spatial filtering as in (Lagunas et al. 2012b). During simulation, the back walls and side walls are assumed to be perfect reflectors so that the ghosts have more pronounced effect. Only the first-order multipath returns were considered. The effect of the higher order multipath is relatively small that the ghosts' effects are significant or reside outside the scene image (Abdalla et al. 2018). Hence, higher order multipath returns were not considered. The scene image resolution was 64×64 pixels.

To quantify the performance, Signal to Clutter Ratio (SCR) and Relative Clutter Peak (RCP) were used. These performance metrics are commonly used in TWRI. Similar performance measures were used in Tang and Nguyen (2020), Tang et al. (2020). The SCR tells how the target can be easily distinguished from the surrounding clutters.

Therefore, high values of SCR signify the easiness of distinguishability of the target in the presence of clutters. On the other hand, small RCP values indicate the probability of correct target detection is highly reduced and the rate of force alarm will increase.

For target detection capability, the precision is used as a performance measure. The precision is the ratio of the number of reconstructed true targets to the sum of true targets and clutters within the imaging region. The lower the precision threshold, the better is the reconstruction method.

The SCR and RCP were evaluated at different noise environments, number of targets, and data volume. To determine the performance of the methods when the scene is perturbed by nose, additive white Gaussian noise (AWGN) was added to the measurement. The results were averaged over 100 Monte Carlo runs for each SNR value.

Results and Discussions

The images formed using one-third of the frequency bins and one-third of the radar locations, which accounts for 11.10% of the total data volume for each method, are shown in Figure 5 (b)-(d). Figure 5 (a) shows the original scene and Figure 5 (b)-(d) show the final images for the three approaches: duo subarray, hybrid, and sparse array, respectively. It can be seen that the ghosts were eliminated and the true targets can be clearly visible in the final images.

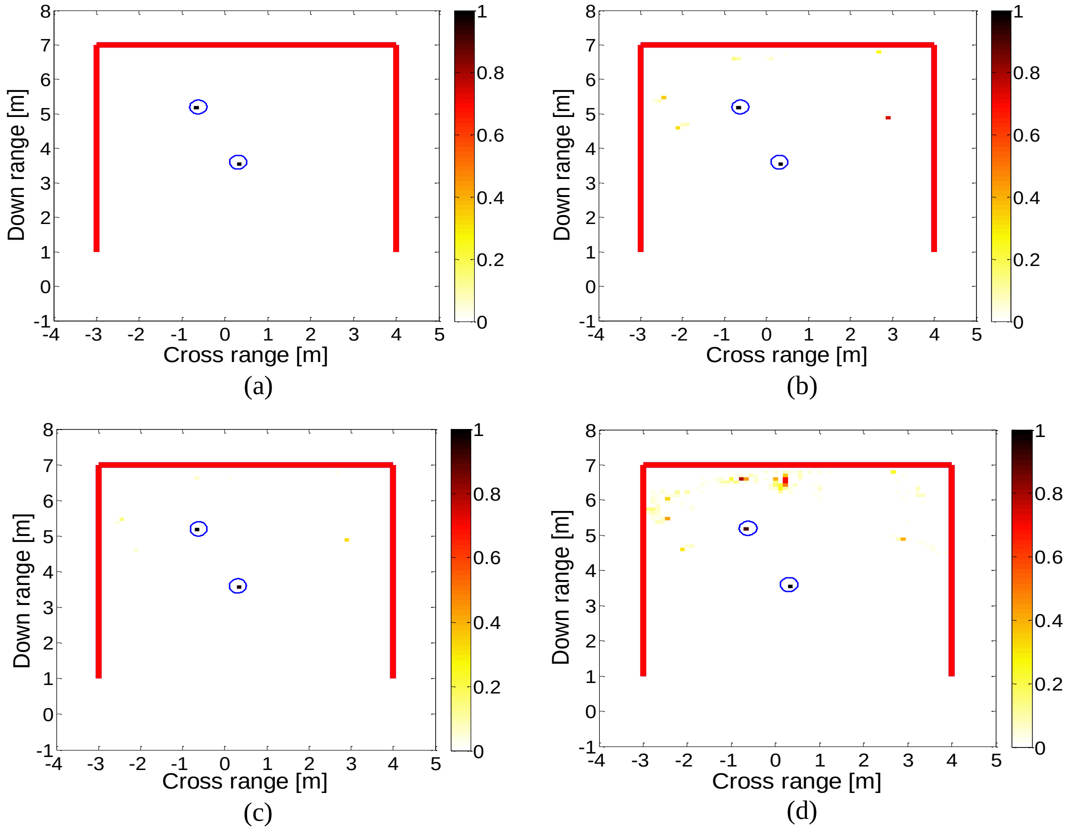

Figure 5: Image reconstruction (a) original scene, (b) Duo-subarray final image, (c) Hybrid final image, and (d) Pythagorean-based displaced subarray.

Simulation results indicate that the hybrid approach gives high values of SCR, while PDSA registered the lowest SCR values. This suggests that the hybrid method is more noise resistant than the duo subarray and PDSA counterpart. The performance graphs are indicated in Figure 6 and Figure 7. Figure 6 (a) shows the performance of various methods in terms of SCR values at different values of Signal to Noise Ratio (SNR), Figure 6 (b) shows the RCP values at different SNR levels. Figure 7 shows the degree to which the reconstructed image resembles the true target, using precision.

To determine the performance as the number of targets increase, we evaluated the methods for the case of single target and two targets. Increasing the number of targets makes the scene less sparse. In either case, the SCR and RCP values were determined. The results indicate that multiple subarray employing duo subarray gives high SCR and RCP values.

Table 1 summarizes the performance for single target and two targets scenarios. When data volume increases, the results suggest that multiple subarray employing duo subarray gives high SCR and RCP values as compared to the other methods. The performance results for 11.10% and 16.67% of the data volumes are presented in Table 2.

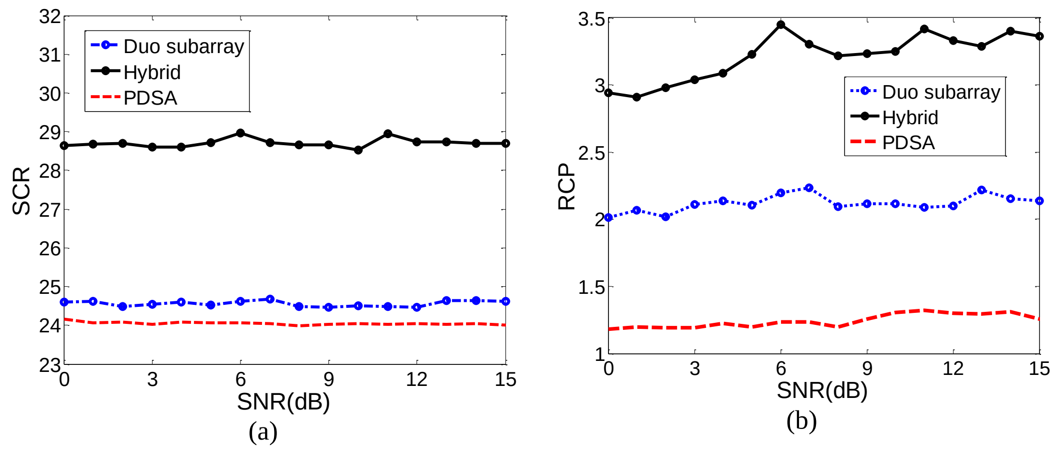

Figure 6: Performance metrics at different SNR: (a) SCR, and (b) RCP.

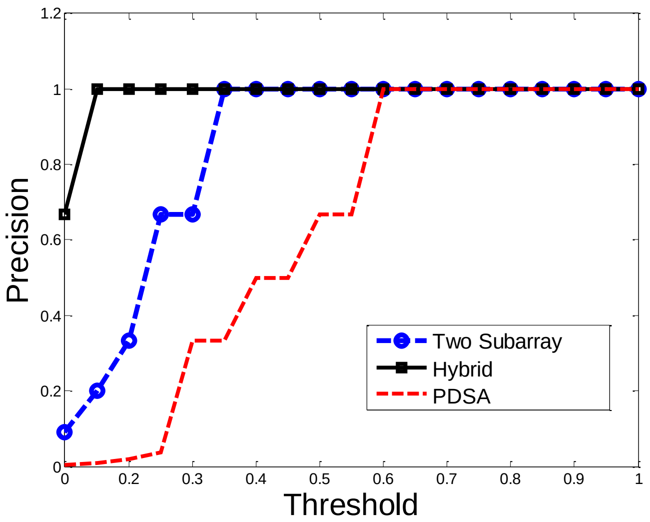

Figure 7: Variation of precision with threshold values.

Table 1: SCR and RCP at varying number of targets

Modality		Single target		Two targets	
		SCR	RCP	SCR	RCP
Multiple subarray:	Duo subarray	68.52	8.63	67.09	7.43
Hybrid		78.92	8.32	66.60	7.11
Sparse array:	PDSA	65.29	8.65	49.96	4.88

Table 2 : SCR and RCP at varying data volume

Modality		11.1% Data volume		16.67% Data volume	
		SCR	RCP	SCR	RCP
Multiple subarray:	Duo subarray	67.71	7.45	72.76	8.88
Hybrid		69.09	9.69	70.52	6.06
Sparse array:	PDSA	60.18	6.54	44.88	2.81

Conclusion

The performance of three strategies under aspect dependent based ghost suppression, namely, multiple subarray, hybrid subarray and sparse array were evaluated. The evaluation considered noisy environment, different numbers of targets in a scene and varying data volumes. It was found that the hybrid subarray was robust to noise, hence suitable under noisy environments. When the scene sparsity is relatively low or high data volume is considered, multiple subarray with duo subarray becomes the best method. Thus, this method can be used when a scene contains multiple targets or extended targets. As an extension of this work, Aspect Dependent Ghost Suppression for extended target is underway.

Acknowledgement

This work was funded by the University of Dar es Salaam Competitive Projects, through the directorate of research, award number COICT-ETE 19048, and was also partially funded by the Tanzania Meteorological Authority (TMA).

References

Abdalla AT 2018 Through-the-wall radar imaging with compressive sensing: theory , practice and future trends-a review. *Tanz. J. Sci.* 44(3): 12–30.

Abdalla AT, Alkhodary MT and Muqaibel AH 2018 Multipath ghosts in through-the-wall radar imaging: challenges and solutions. *ETRI J.* 40(3): 376–388.

Abdalla AT and Muqaibel AH 2016 Multiple target sparse reconstruction in TWRI utilizing ghost’s aspect dependence feature. RFM 2015 - 2015 IEEE International RF and Microwave Conference. Kuching, 280–284.

Abdalla AT, Muqaibel AH and Al-dharrab S 2015 Aspect dependent multipath ghost suppression in TWRI under compressive sensing framework. Proceedings of the Int. Conf. Comm., Sig. Process. and their App. (ICCSPA15). Sharjah,1–6.

Amin MG and Ahmad F 2014 Through-the-wall radar imaging: theory and applications. In: Academic Press Library in Signal Processing. Communications and Radar Signal Processing vol. 2 (pp.857-909), Elsevier Masson SAS .

An Q, Hoorfar A, Zhang W, Li S and Wang J 2019 Range coherence factor for down range sidelobes suppression in radar imaging through multilayered dielectric media. IEEE Access. 7: 66910–66918.

Gennarelli and Soldovieri F 2015 Multipath ghosts in radar imaging: physical insight and mitigation strategies. IEEE *J. Select. Topics Appl. Earth Observ. Remote Sensing* 8(3): 1078–1086.

Granström K and Bramstång J 2019 Bayesian smoothing for the extended object random matrix model. *IEEE Trans. Sign. Proces.* 67(14): 3732–3742.

Guo, Yang X, Cui G, Song Y and Kong L 2018 Multipath ghost suppression for through-the-wall imaging radar via array rotating. *IEEE Geosci. Remote Sens. Lett.* 15(6): 868-872.

Jia Y, Song R, Chen S, Wang G, Guo Y, Zhong X and Cui G 2019a Multipath ghost suppression based on generative adversarial nets in through-wall radar imaging. *Electronics* 8(6): 626.

Jia Y, Song R, Chen S, Wang G and Yan C 2019b Preliminary results of multipath ghost suppression based on generative adversarial nets in TWRI. 2019 IEEE 4th International Conference on Signal and Image Processing. Wuxi, 208–212.

Jin T and Yarovoy A 2015 A Through-the-wall radar imaging method based on a realistic model. *Int. J. Antenn. Propag.* 2015: 1-8.

Lagunas E, Amin MG, Ahmad F and Najar M 2012a Compressive sensing for through wall radar imaging of stationary scenes using arbitrary data measurements, 11th International Conference on Information Science, Signal Processing and Their Applications. Montreal, 1347–1352.

Lagunas E, Amin MG, Ahmad F and Nájar M 2012b Wall mitigation techniques for indoor sensing within the compressive sensing framework. In Proceedings of the IEEE 7th Sensor Array and Multichannel Signal Processing Workshop (SAM). Hoboken, 213-216.

Leigsnering M, Ahmad F, Amin M and Zoubir A 2014a Multipath exploitation in through-the-wall radar imaging using sparse reconstruction. *IEEE Transactions on Aerospace and Electronic Systems* 50(2): 920–939.

Leigsnering M, Amin M, Ahmad F and Zoubir AM 2014b Multipath exploitation and suppression for SAR imaging of building interiors: An overview of recent advances. *IEEE Sign. Proces. Magaz.* 31(4): 110–119.

Leigsnering M, Ahmad F, Amin MG and Zoubir AM 2016 Parametric dictionary learning for sparsity-based TWRI in multipath environments. *IEEE Trans. Aerospace Electron. Syst* 52(2): 532–547.

Li Z, Kong L, Jia Y, Zhao Z and Lan F 2013 A novel approach of multi-path suppression based on sub-aperture imaging in through-wall-radar imaging. IEEE National Radar Conference - Proceedings: Ottawa, 4–7.

Lim Y and Nam S 2014 Target-to-clutter ratio enhancement of images in through-the-wall radar using a radiation pattern-based delayed-sum algorithm. *J. Electromagn. Eng. Sci.* 14(4): 405–410.

Liu J, Kong L, Yang X and Liu QH 2016 First-order multipath ghosts' characteristics and suppression in MIMO through-wall imaging. *IEEE Geosci. Remote Sens. Lett.* 13(9): 1315–1319.

Ma Y, Hong H and Zhu X 2018 Interaction multipath in through-the-wall radar imaging based on compressive sensing. *Sensors* 18(2): 549.

Muqaibel AH, Abdalla AT, Alkhodary MT and Al-Dharrab S 2017a Aspect-dependent efficient multipath ghost suppression in TWRI with sparse reconstruction. *Int. J. Microw. Wireless Technol.* 9(9): 1839–1852.

Muqaibel AH, Abdalla AT, Alkhodary MT and Alawsh SA 2017b Through-the-wall radar imaging exploiting Pythagorean apertures with sparse reconstruction. *Digit. Sign. Proces.* 61: 86–96.

Qu L, An S and Sun Y 2019 Cross validation based distributed greedy sparse recovery for multiview through-the-wall radar imaging. *Int. J. Anten. Propag.* 2019: 1-9.

Shi X, Wang C and Zheng C 2020 Wall clutter mitigation based on spread spectrum radar in through-the-wall radar. *Microw. Optic. Technol. Lett.* 62(5): 1987–1990.

Tan Q, Leung H, Song Y and Wang T 2014 Multipath ghost suppression for through-the-wall radar. *IEEE Trans. Aerospace Electron. Syst.* 50(3): 2284–2292.

Tan Q and Song Y 2010 A new method for multipath interference suppression in through-the-wall UWB radar imaging. Proceedings - 2nd IEEE International Conference on Advanced Computer Control. Shenyang, 5(2): 535–540.

Tang VH, Bouzerdoum A and Phung SL 2020 Compressive radar imaging of stationary indoor targets with low-rank plus jointly sparse and total variation regularizations. *IEEE Trans. Image Proces.* 29: 4598–4613.

Tang VH, Bouzerdoum A, Phung SL and Bin H 2020 A variational bayesian approach for multichannel through-wall radar imaging with low-rank and sparse priors. 2020 IEEE International Conference on Acoustics, Speech and Signal Processing (ICASSP). Barcelona, 2523–2527.

Tivive FHC, Bouzerdoum A and Abeynayake C 2019 GPR Target detection by joint sparse and low-rank matrix decomposition.

IEEE Trans. Geosci. Remote Sens. 57(5): 2583–2595.

Tseng YH, Chen YH and Lu CW 2017 Adaptive integration of the compressed algorithm of CS and NPC for the ECG signal compressed algorithm in VLSI implementation. *Sensors* 17(10): 2288.

Tang H and Nguyen VG 2019 A rank-deficient and sparse penalized optimization model for compressive indoor radar imaging. Proceedings-2019 3rd International Conference on Recent Advances in Signal Processing, Telecommunications and Computing, SigTelCom 2019. Hanoi, 102: 48–52.

Tang H and Nguyen VG 2020 A rank-deficient and sparse penalized optimization model for compressive indoor radar imaging. *REV J. Electron. Commun.* 10(1-2).

Webster JG, Stanković S, Stanković L, Orović I and Daković M 2017 Sparse Signal Reconstruction-Introduction. Wiley Encyclopedia of Electrical and Electronics Engineering 1(1): 1–21.

Yan D, Cui G, Guo S, Kong L, Yang X and Liu T 2016 Multipath ghosts location and sub-aperture based suppression algorithm for TWIR. 2016 IEEE Radar Conference. Philadelphia, 3–6.

Yang J, Jin T, Xiao C and Huang X 2019 Compressed sensing radar imaging: Fundamentals, challenges, and advances. *Sensors* 19(14): 3100.

Yao X, Cui G, Kong L, Liu J, Luo W and Jia Y 2014 Building layout imaging with spatial filtering based on image optimization. IEEE National Radar Conference - Proceedings. Cincinnati, 1094–1097.

Yoon YS and Amin MG 2009 Spatial filtering for wall-clutter mitigation in through-the-wall radar imaging. *IEEE Transactions on Geosci. Remote Sens.* 47(9): 3192–3208.

Zhang W, Amin MG, Ahmad F, Hoorfar A and Smith GE 2012 Ultrawideband impulse radar through-the-wall imaging with compressive sensing. *Int. J. Antenn. Propag.* 2012: 1–11.